3 Wavelet Galerkin and wavelet collocation method in moving boundary problem with temperature dependent thermal physical properties

3.1 Introduction

Heat transfer problems involving phase change have wide applications in many fields of scientific and technological endeavour and have been focus of extensive study by Flemings (1974) and Crank (1984). The mathematical model for such problems are the system of partial differential equation of parabolic type with moving boundaries. Due to the moving boundary condition these problems are nonlinear even its simplest form. The exact solution of such problems is possible in similarity form only in limited case. Briozzo *et al.* (2007) studied the existence of an exact solution for one phase Stefan problem with nonlinear thermal coefficients using Tirskii's method. An analytical study of the solidification in semi infinite porous medium was given by Rai and Rai (1992). Tirskii (1959) studied a two exact solution of Stefan's nonlinear problem. If thermal conductivity and specific heat of two regions are different and temperature dependent, we have a double nonlinear problem. Such nonlinear problems cannot be solved exactly. Many approximate and numerical methods have been used for solution of such problems (Ang *et al.* (1998); Cho and Sunderland (1974); Fredrick and Greif (1985); Goodman and Shea (1960); Prud and Hung (1989); Singh *et al.* (2011)). Goodman (1958) used a heat-balance integral method to solve the phase change problem. The optical exponent heat balance and refined integral method was used by Myers (2010) to solve Stefan problems. Numerical solution of moving boundary problem in a finite domain was given by Rai and Singh (1998). Rajeev *et al.* (2009a) used numerical solution for solving moving boundary problem with variable latent heat. Rai and Singh (1998) used the variational iteration method to solve inverse one-phase Stefan problem. Savovic and Caldwell (2009) solved the Stefan problem with time-dependent boundary condition by using variable space grid method. Singular perturbation theory for solving melting or freezing problems in finite domains was used by Weinbaum and Jiji (1977).

There are two types of solidification problems that have been considered: one where the liquid is initially above the freezing temperature and in which the temperature in both solid and liquid must be determined (two-phases). Oliver and Sunderland (1987); Rai and Singh (1998); Singh *et al.* (2011) solved such problems and the other where the liquid is always at the freezing temperature (one-phase) studied by Briozzo *et al.* (2007); Natale and Tarzia (2003); Rai and Singh (1998); Rajeev *et al.* (2009b); Yang *et al.* (2003). For two phases problem, the significant progress in a finite domain was reported by Weinbaum and Jiji (1977). Cooling process was by an isothermal wall below freezing temperature while the other end was either adiabatic or isothermal. The problem was solved by method of matched asymptotics. Oliver and Sunderland (1987) considered a two phases moving boundary problem in which thermal conductivity and specific heat of two regions varies linearly with temperature. This problem was solved using a numerical method. Singh *et al.* (2011) solved the same problem by using variational iteration method when thermal conductivity and specific heat of two regions varies (1) linearly and (2) exponentially with temperature. No solution is provided when thermal conductivity and specific heat of two regions varies with temperature in a general manner and their densities are also different. To the best of authors knowledge solution of the two phases moving boundary problem with temperature dependent thermal conductivity and specific heat and different densities of two regions has not been solved yet using wavelet Galerkin or wavelet collocation method. In this study, the proposed method is used to obtain the solution of a two phases moving boundary problem when thermal conductivity and specific heat of two regions are temperature dependent and densities of two regions are different. The two regions moving boundary problem of partial differential equation have been transferred into a two regions fixed boundary problem of nonlinear ordinary differential equations. Further, the wavelet Galerkin and wavelet collocation method have been used to solve them.

3.2 Formulation of Mathematical Model

A semi infinite medium consisting of a melt is initially at a temperature T_i which is slightly above the freezing temperature of the melt T_f. The surface $r = 0$ is kept at a temperature T_0 slightly below the freezing temperature of the material. The freezing starts at the surface $r = 0$ and the solid-liquid interface $r = s(t)$ moves in the positive r- direction. The dynamics of freezing can be described by the following differential equations:

$$[\rho_1 c_1(T_1)] \frac{\partial T_1}{\partial t} = \frac{\partial}{\partial r}\left[K_1(T_1)\frac{\partial T_1}{\partial r}\right],\ 0 < r < s(t),\ t > 0, \tag{3.1}$$

$$[\rho_2 c_2(T_2)] \frac{\partial T_2}{\partial t} + (\rho_1 - \rho_2)c_2(T_2)\frac{ds}{dt}\frac{\partial T_2}{\partial r} = \frac{\partial}{\partial r}\left[K_2(T_2)\frac{\partial T_2}{\partial r}\right],\ r > s(t),\ t > 0, \tag{3.2}$$

subjected to the initial and boundary conditions

$$T_1(r, 0) = T_i, \tag{3.3}$$

$$T_1(0, t) = T_0. \tag{3.4}$$

On the moving interface, the condition of temperature continuity and energy balance equation are

$$T_1(s(t), t) = T_2(s(t), t) = T_f, \tag{3.5}$$

$$K_1(T_1)\frac{\partial T_1}{\partial r} - K_2(T_2)\frac{\partial T_2}{\partial r} = \rho_1 L \frac{ds(t)}{dt},\ r = s(t), \tag{3.6}$$

$$s(0) = 0. \tag{3.7}$$

respectively. As $r \to \infty$ the temperature of material is equal to initial temperature i.e.,

$$\lim_{r\to\infty} T_2(r, t) = T_i. \tag{3.8}$$

The thermal conductivity and specific heat in two regions varies with temperature and are assumed to be:

$$
\begin{aligned}
&K_1 = K_{01} g_1(\theta_1), \\
&K_2 = K_{02} g_2(\theta_2), \\
&c_1 = c_{01} f_1(\theta_1), \\
&c_2 = c_{02} f_2(\theta_2),
\end{aligned} \tag{3.9}
$$

respectively.

3.2.1 Dimensionless Analysis

Introducing the dimensionless variables and similarity criteria

$$
\begin{aligned}
&\theta_k = \frac{T_k - T_0}{T_i - T_0},\ k = 1, 2, f,\ a_{12} = \frac{a_{02}}{a_{01}},\ a_{01} = \frac{K_{01}}{c_{01}\rho_1},\ a_{02} = \frac{K_{02}}{c_{02}\rho_2},\ K_{12} = \frac{K_{02}}{K_{01}} \\
&\rho_{21} = \frac{\rho_2}{\rho_1},\ Fo = \frac{a_{01} t}{l^2},\ Ste = \frac{c_{01}(T_i - T_0)}{L},\ y = \frac{r}{l},\ \lambda = \frac{s(t)}{l},
\end{aligned} \tag{3.10}
$$

and using transformation

$$
x = \frac{y}{\lambda},\ \lambda = 2\lambda_0 \sqrt{F_0}, \tag{3.11}
$$

the system of Eqs. (3.1 - 3.8) reduce in to the form

$$
\frac{d}{dx}\left[g_1(\theta_1)\frac{d\theta_1}{dx}\right] + 2\lambda_0^2 x f_1(\theta_1)\frac{d\theta_1}{dx} = 0,\ 0 < x < 1, \tag{3.12}
$$

$$
\frac{d}{dx}\left[g_2(\theta_2)\frac{d\theta_2}{dx}\right] + \frac{2\lambda_0^2}{a_{12}} f_2(\theta_2)(1 + x - \rho_{21})\frac{d\theta_2}{dx} = 0,\ x > 1, \tag{3.13}
$$

$$
\theta_1(0) = 0, \tag{3.14}
$$

$$
\theta_1(1) = \theta_2(1) = \theta_f. \tag{3.15}
$$

Interface equation is

$$
g_1(\theta_1)\frac{d\theta_1}{dx} - K_{12} g_2(\theta_2)\frac{d\theta_2}{dx} = \frac{2\lambda_0^2}{Ste},\ x = 1, \tag{3.16}
$$

$$
\lim_{x\to\infty} \theta_2(x) = 1. \tag{3.17}
$$

Under the transformation

$$
z = e^{1-x}, \tag{3.18}
$$

the region $[1, \infty)$ reduces into region $[0, 1]$, the Eqs. (3.13), (3.15 - 3.17) reduce in the form of

$$z\frac{d}{dz}\left[g_2(\theta_2)z\frac{d\theta_2}{dz}\right] - \frac{2\lambda_0^2}{a_{12}}f_2(\theta_2)(2 - \rho_{21} - logz)z\frac{d\theta_2}{dz} = 0, \tag{3.19}$$

$$\theta_2(1) = \theta_f, \tag{3.20}$$

$$\lim_{z\to 0}\theta_2(z) = 1, \tag{3.21}$$

$$g_1(\theta_1)\frac{d\theta_1}{dx} - K_{12}g_2(\theta_2)\frac{d\theta_2}{dx} = \frac{2\lambda_0^2}{Ste},\ x = 1, \tag{3.22}$$

$$\text{where } \frac{d\theta_2}{dx} = -z\frac{d\theta_2}{dz},\ z = 1. \tag{3.23}$$

3.3 Wavelet Galerkin and wavelet Collocation Method

To obtain the solution of system of Eqs. (3.12), (3.14), (3.15) and Eqs. (3.19)-(3.23), we will use wavelet Galerkin and wavelet collocation method.

Phase (1)

Let us assume

$$\frac{d^2\theta_1}{dx^2} = C_1^T\psi_1(x), \tag{3.24}$$

where Ledendre wavelets $\psi_1(x)$ and unknown vector C_1 of order $2^{k-1}M \times 1$ are defined as

$$\begin{aligned}\psi_1(x) = \quad & [\psi_{10}(x), \psi_{11}(x), \ldots, \psi_{1M-1}(x), \psi_{20}(x), \psi_{21}(x), \ldots, \psi_{2M-1}(x), \ldots, \psi_{2^{k-1}0}(x),\\ & \psi_{2^{k-1}1}(x), \psi_{2^{k-1}2}(x), \ldots, \psi_{2^{k-1}M-1}(x)]^T.\\ C_1 = \quad & [c_{10}^1, c_{11}^1, ..., c_{1M-1}^1, c_{20}^1, c_{21}^1, ..., c_{2M-1}^1, c_{2^{k-1}0}^1, c_{2^{k-1}1}^2, ..., c_{2^{k-1}M-1}^1]^T.\end{aligned}$$

Integrating Eq. (3.24) from 0 to x and using Eq. (1.92) we get

$$\frac{d\theta_1}{dx} - \frac{d\theta_1(0)}{dx} = C_1^T P\psi_1(x), \tag{3.25}$$

where P is operational matrix of integration of order $2^{k-1}M \times 2^{k-1}M$ defined in Eq. (1.93). Again integrating Eq. (3.25) from 0 to x, we get

$$\theta_1(x) = \frac{d\theta(0)}{dx}d^T P\psi_1(x) + C_1^T P^2\psi_1(x), \tag{3.26}$$

where d is a vector coefficient determine by $< \psi_{nm}, d^T\psi_1(x) > = < \psi_{nm}, 1 >$, where ψ_{nm} is defined in Eq. (1.87). Put $x = 1$ in Eq. (3.26) and using boundary condition defined in Eq. (3.15), we get

$$\frac{d\theta_1(0)}{dx} = \theta_f - C_1^T P^2 \psi_1(1), \tag{3.27}$$

Now, substitute Eq. (3.27) in Eq. (3.26) we get

$$\theta_1(x) = (\theta_f - C_1^T P^2 \psi_1(1)) d^T P \psi_1(x) + C_1^T P^2 \psi_1(x). \tag{3.28}$$

Phase (2)

Let us assume

$$\frac{d^2\theta_2}{dz^2} = C_2^T \psi_2(z), \tag{3.29}$$

where, Ledendre wavelets $\psi_2(z)$ and unknown vector C_2 of order $2^{k-1}M \times 1$ are defined as

$$\begin{aligned} \psi_2(z) = \quad & [\psi_{10}(z), \psi_{11}(z), \psi_{12}(z), \ldots, \psi_{1M-1}(z), \psi_{20}(z), \psi_{21}(z), \ldots, \psi_{2M-1}(z), \ldots, \\ & \psi_{2^{k-1}0}(z), \psi_{2^{k-1}1}(z), \ldots, \psi_{2^{k-1}M-1}(z)]^T. \\ C_2 = \quad & [c_{10}^2, c_{11}^2, ..., c_{1M-1}^2, c_{20}^2, c_{21}^2, ..., c_{2M-1}^2, c_{2^{k-1}0}^2, c_{2^{k-1}1}^2, ..., c_{2^{k-1}M-1}^2]^T. \end{aligned}$$

Integrating the Eq. (3.33) from 0 to z two times and using Eq. (1.92) and boundary condition defined in Eq. (1.20), we get

$$\theta_2(z) = 1 + (\theta_f - 1 - C_2^T P^2 \psi_2(1) + C_2^T P \psi_2(z)) d^T P \psi_2(z) + C_2^T P^2 \psi_2(z). \tag{3.30}$$

Particular cases: Here we consider three particular cases as follows:

Case 1

When thermal conductivity and specific heat are temperature independent we take,

$$g_1(\theta_1) = f_1(\theta_1) = 1. \tag{3.31}$$

Using the Eqs. (3.24), (3.28) in Eq. (3.12) we get the residual

$$R_1(x, \lambda_0, C_1) = C_1^T \psi_1(x) + k_0^T \psi_1(x)((\theta_f - C_1^T P^2 \psi_1(1)) d^T \psi_1(x) + C_1^T P \psi_1(x)), \tag{3.32}$$

where $k_0^T \psi_1(x) = 2\lambda_o^2 x$.

For phase 2, we have used similar process as used in phase 1 for obtaining the residual. We get

$$R_2(z, \lambda_0, C_2) = k_1^T \psi_2(z) C_2^T \psi_2(z) + k_2^T \psi_2(z)(\theta_f - 1 - C_2^T P^2 \psi_2(1) + C_2^T P \psi_2(z)), \tag{3.33}$$

where $k_1^T\psi_2(z) = z, \quad k_2^T\psi_2(z) = (1 - \frac{2\lambda_o^2}{a_{12}}(2 - \rho_{21} - logz))$.

For minimizing these residuals ($R_1(x, \lambda_0, C_1)$ and $R_2(z, \lambda_0, C_2)$), using the Galerkin approach defined in Eq. (1.65). In Galerkin approach, we have taken the test function as Legendre wavelets defined in Eq. (1.87). Therefore, we get the system of linear equations for both the phases as follows:

$$A_1C_1 = B_1, \tag{3.34}$$

and

$$A_2C_2 = B_2. \tag{3.35}$$

Where

$$\begin{aligned}
A_1 = &\quad I - \hat{k_0}d\psi_1^T(1)P^{2T} + \hat{k_0}P^T,\\
A_2 = &\quad \hat{k}_1 - \hat{k}_2d\psi_2^TP^2T + \hat{k}_2d\hat{k}_2^T(1)P^T,\\
B_1 = &\quad \theta_f\hat{k_0}d,\\
B_2 = &\quad (1-\theta_f)\hat{k}_2d.
\end{aligned}$$

A_1, A_2 and B_1, B_2 are known matrices of order $2^{k-1}M \times 2^{k-1}M$ and $2^{k-1}M \times 1$ respectively. I is the identity matrix of order $2^{k-1}M \times 2^{k-1}M$. For determining the unknown vectors $C_j, \ j = 1, 2$ we are using Gauss elimination technique in Eq. (3.34) and Eq. (3.35), provided the determinant A_1, A_2 are not vanishes. Substituting the value of $C_j, \ j = 1, 2$, we obtained the value of θ_1 and θ_2 for phase 1 and phase 2 respectively.

Case 2

When specific heat and thermal conductivity varies exponentially with temperature i.e.,

$$\begin{aligned}
f_1(\theta_1) &= e^{\alpha_1\theta_1},\\
f_2(\theta_2) &= e^{\alpha_2\theta_2},\\
g_1(\theta_1) &= e^{\beta_1\theta_1},\\
g_2(\theta_2) &= e^{\beta_2\theta_2}.
\end{aligned} \tag{3.36}$$

Similarly, the residuals obtained for phase 1 and phase 2 are given as

$$\begin{aligned} R_3(x,\lambda_0,C_1) = \quad & C_1^T\psi_1(x) + \beta_1(\theta_f - C_1^T P^2\psi_1(1) + C_1^T P\psi_1(x))^2 + 2\lambda_0^2 x \times \\ & e^{[(\alpha_1-\beta_1)(\theta_f - C_1^T P^2\psi_1(1)x + C_1^T P^2\psi_1(x))]}(\theta_f - C_1^T P^2\psi_1(1) + C_1^T P\psi_1(x)). \end{aligned} \tag{3.37}$$

$$\begin{aligned} R_4(z,\lambda_0,C_2) = \quad & C_2^T\psi_2(z) + \theta_f - 1 - C_2^T P^2\psi_2(1) + C_2^T P\psi_2(z) + \beta_2 z(\theta_f - 1 - (1) \\ & C_2^T P^2\psi_2 + C_2^T P\psi_2(z))^2 - \frac{2\lambda_0^2}{a_{12}} e^{[(\alpha_2-\beta_2)(1+(\theta_f-1-C_2^T P^2\psi_2(1))z + C_2^T P^2\psi_2(z))]} \\ & (\theta_f - C_2^T P^2\psi_2(1) C_2^T P\psi_2)(2 - log(z) - \rho_{21}). \end{aligned} \tag{3.38}$$

Case 3

When specific heat and thermal conductivity varies linearly with temperature i.e.,

$$\begin{aligned} f_1(\theta_1) &= 1 + \alpha_1\theta_1, \\ f_2(\theta_2) &= 1 + \alpha_2\theta_2, \\ g_1(\theta_1) &= 1 + \beta_1\theta_1, \\ g_2(\theta_2) &= 1 + \beta_2\theta_2. \end{aligned} \tag{3.39}$$

Similarly, the residuals obtained for phase 1 and phase 2 are given as

$$\begin{aligned} R_5(x,\lambda_0,C_1) = \quad & C_1^T\psi_1(x) + \beta_1(\theta_f - C_1^T P^2\psi_1(1)) x C_1^T\psi_1(x) + \beta_1 C_1^T P^2\psi_1(x) C_1^T\psi_1(x) \\ & +\beta_1(\theta_f - C_1^T P^2\psi_1(1) + C_1^T P\psi_1(x))^2 + 2\lambda_0^2 x^2\alpha_1(\theta_f - C_1^T P^2\psi_1(1))^2 \\ & +2\lambda_0^2 x(\theta_f - C_1^T P^2\psi_1(1) + C_1^T P\psi_1(x)) + 2\lambda_0^2 x\alpha_1(\theta_f - C_1^T P^2\psi_1(1)) \times \\ & C_1^T P\psi_1(x) + 2\lambda_0^2 x^2\alpha_1(\theta_f - C_1^T P^2\psi_1(1)) C_1^T P\psi_1(x) + 2\lambda_0^2 x\alpha_1 C_1^T P\psi_1(x). \end{aligned} \tag{3.40}$$

$$\begin{aligned} R_6(z,\lambda_0,C_2) = \quad & zC_2^T\psi_2(z) + \beta_2 z(1 + (\theta_f - 1 - C_2^T P^2\psi_2(1))z + C_2^T P^2\psi_2(z)) C_2^T\psi_2(z) \\ & +(\theta_f - 1 - C_2^T P^2\psi_2(1)) + C_2^T P\psi_2(z) + \beta_2(z(\theta_f - 1 - C_2^T P^2\psi_2(1)) \\ & +C_2^T P^2\psi_2(z) + 1) \times (\theta_f - 1 - C_2^T P^2\psi_2(1) + C_2^T P\psi_2(z)) \\ & -\frac{2\lambda_0^2}{a_{12}}(2 - \rho_{21} - logz)(\theta_f - 1 - C_2^T P^2\psi_2(1) + C_2^T P\psi_2) \\ & +\beta_2 z(\theta_f - 1 - C_2^T P^2\psi_2(1) + C_2^T P\psi_2)^2 - \frac{2\lambda_0^2}{a_{12}}(2 - \rho_{21} - logz)\alpha_2 \times \\ & (1 + (\theta_f - 1 - C_2^T P^2\psi_2(1) z) + C_2^T P^2\psi_2(z)) \\ & (\theta_f - 1 - C_2^T P^2\psi_2(1) + C_2^T P\psi_2(z)). \end{aligned} \tag{3.41}$$

In both the cases, we have taken $2^{k-1}M$ collocation points x_{nm} in interval $(0,1)$ such that

$$R_i(x_{nm}, \lambda_0, C_j) = 0, \;\; i = 3, 4, 5, 6, \;\;\; j = 1, 2.$$

Therefore, we get $2^{k-1}M$ system of nonlinear equations for each i. For determining the unknown vector C_j, we are using the Newton Raphson method. Substituting the value of C_j in Eqs. (3.28), (3.30), we get $\theta_1$and θ_2 for both phases respectively.

3.3.1 Moving Layer Thickness

For determining the moving layer thickness λ_0 for each cases, substitute the obtained θ_1, θ_2 in Eq. (3.22) we get non linear equation in λ_0 and solve it by Newton-Raphson method.

3.4 Convergence Analysis

Let $\theta(x)$ be a continuous function defined on interval $[0,1]$ and let $\theta_N(x)$ be an approximate solution of Eq. (3.28) which can be written in the form of

$$\theta_N(x) = \sum_{n=0}^{N-1} a_n \psi_{1n}. \tag{3.42}$$

Where a_n is an unknown constant and $\{\psi_{1n} : n = 0, 1, 2........N-1\}$ be an orthonormal set of Legendre wavelets.
Let us assume that

$$\|\theta(x) - \theta_N(x)\|_2 = \|E(x)\|_2, \tag{3.43}$$

where,

$$E(x) = \sum_{n=N}^{\infty} (|a_n|^2)^{1/2},$$

and a_n is defined as

$$a_n = \int_0^1 \theta(x)\psi_{1n} dx.$$

Therefore,

$$\|\theta(x) - \theta_N(x)\|_2 \leq M \int_0^1 \psi_{1n} dx, \tag{3.44}$$

where, $M = \sup \theta(x),\ x\epsilon[0,1]$. Since,

$$\int_0^1 \psi_{1n} dx = \begin{cases} 1, n = 0 \\ 0, \quad otherwise. \end{cases} \tag{3.45}$$

From Eq. (3.44) and (3.45), we get $\|\theta(x) - \theta_n(x)\|_2 = 0$. Hence, it shows that $\|E(x)\|_2 = 0$ for large value of N.

3.5 Numerical Computation and Disscussion

In case (1), the exact solution of Eqs. (3.12 - 3.13) comes out to be

$$\theta_1 = \theta_f \frac{erf(\lambda_0 x)}{erf(\lambda_0)} \tag{3.46}$$

$$\theta_2 = \frac{1}{2} + \frac{1}{2}\left[\frac{erf(\lambda_0 x) - erf(\lambda_0)}{1 - erf(\lambda_0)}\right], \tag{3.47}$$

where, erf is error function and defined as

$$erf(x) = \frac{2}{\sqrt{\pi}} \int_0^x e^{-t^2} dt. \tag{3.48}$$

The computation has been made and the results thus obtained by present method are compared with exact result. Fig. (3.1) and Fig. (3.2) show the moving layer thickness (λ) and temperature distribution respectively in two regions which are exactly the same as the exact result for case (1). During the solidification process, the motion of moving front is proportional to the parameter λ_0 which is expressed by Eq. (3.11) and also depend on dimensionless parameters such as K_{12}, ρ_{21}, Ste, specific heat coefficients α_1, α_2 and thermal conductivity coefficients β_1, β_2. Fig. (3.3) and Fig. (3.4) also show the temperature distribution in two regions for case (2) and case (3) respectively. From Figs. (3.3) and Fig. (3.4), we observed that the dimensionless temperatures increases and then become constant as dimensionless space co-ordinate increases. The dimensionless moving layer thickness increases as the ratio of densities of liquid region and solid region ρ_{21} and dimensionless time Fo increases, which is shown in Fig. (3.5). The density difference between the solid and liquid is one of the four factors that can lead to macro segregation in ingots. During the solidification of $Al - Cu$ alloys the copper rejected into the liquid raises its density and causes it to settle down (Porter (2009)). The effect of variability of the ratio of thermal conductivity of two regions on moving interface is shown in Fig. (3.6). From this Fig. we observed that, the dimensionless moving layer thickness decreases as ratio of thermal conductivity (K_{12}) increases. A higher value of K_{12} is because of lower conductivity of solid region relative to liquid region and slower freezing as shown in Fig. (3.6). The effect of variability of specific heat with temperature is shown in Fig. (3.7) and Fig. (3.8) for both cases. As α_1, α_2 increases, the thickness of moving interface decreases. The effect of variability of thermal conductivity with temperature is shown in Fig. (3.9) and Fig. (3.10). As β_1, β_2 increases, the thickness of moving interface increases. Further, the effect of thermal conductivity is more pronounced than heat capacity. The Stefan number signifies the importance of sensible heat relative to the latent heat. The higher value of Stefan number, the higher value of heat capacity or lower value of latent heat, the faster is the freezing as shown in Fig. (3.11). For large Stefan numbers, the dimensionless moving layer thickness approaches a constant value. In case of solidification of super cooled melt Stefan number is large and because of this the solidification process may be so rapid that liquid molecules have no time to rearrange themselves into the usual crystal structure and instead form an amorphous solid structure that is reminiscent of the liquid phase. For this reason solids formed from a super cooled liquid have been referred to as liquids on pause (NASA (2012)). As the Stefan number decreases, the dimensionless moving layer thickness decreases. At the low values of Stefan number, the variation in thermal conductivity is important, but the effects of specific heats diminish.

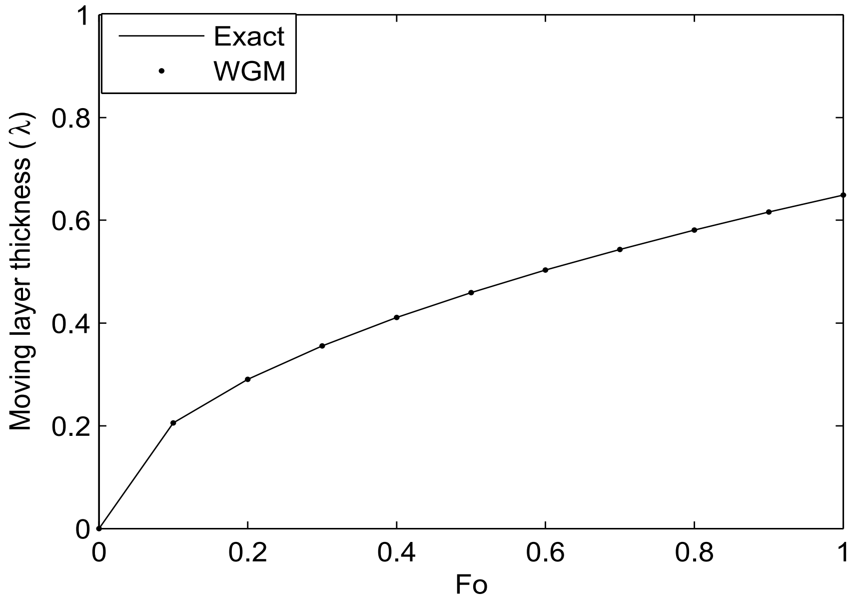

$a_{12} = 1,\ \theta_f = 0.5,\ \rho_{21} = 1,\ \alpha_1 = \alpha_2 = \beta_1 = \beta_2 = 0$

Figure 3.1: Compare the exact result of moving layer thickness (λ) with WGM.

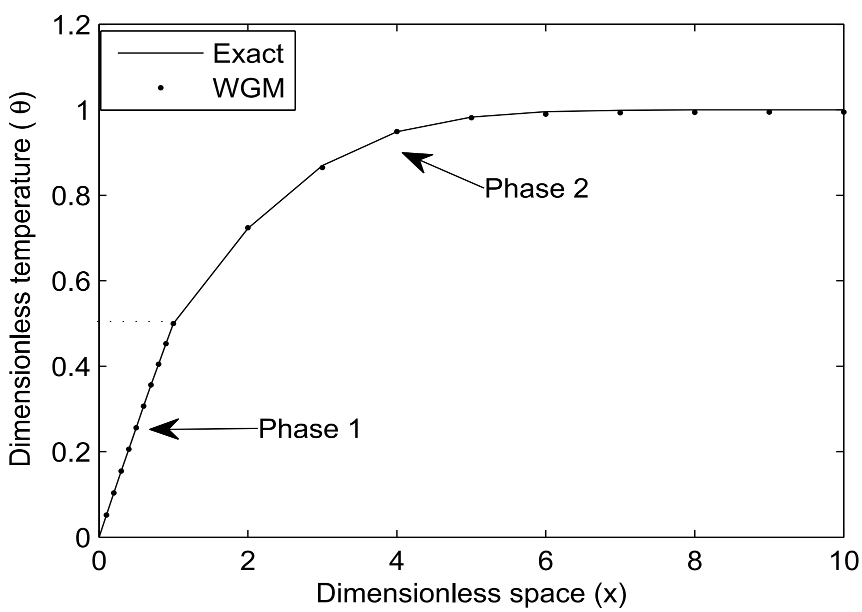

$a_{12} = 1,\ \theta_f = 0.5,\ \rho_{21} = 1,\ \lambda_0 = 0.3246,\ Ste = 1$

Figure 3.2: Compare the exact result of dimensionless temperature distribution (θ) of phase 1 and phase 2 with WGM.

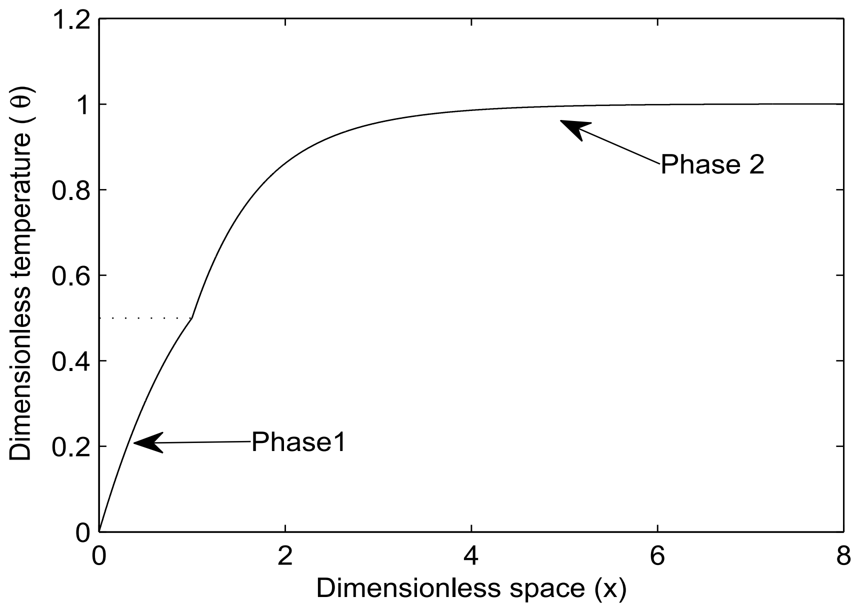

$a_{12} = 1$, $\theta_f = 0.5$, $\rho_{21} = 1$, $\alpha_1 = \alpha_2 = \beta_1 = \beta_2 = 1$, $\lambda_0 = 0.06486$, $Ste = 1$

Figure 3.3: Dimensionless temperature distribution (θ) of phase 1 and phase (2).

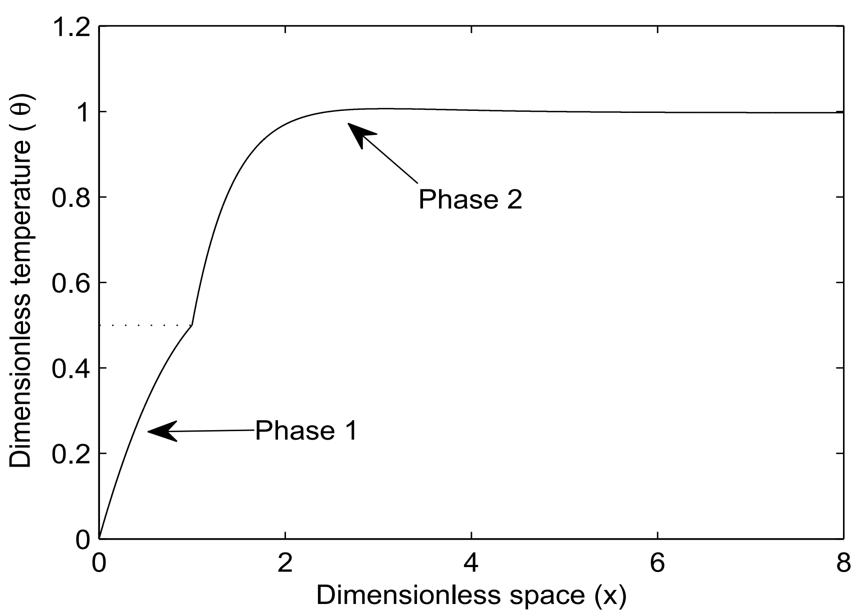

$a_{12} = 1$, $\theta_f = 0.5$, $\rho_{21} = 1$, $\alpha_1 = \alpha_2 = \beta_1 = \beta_2 = 1$,$\lambda_0 = 0.08324$, $Ste = 1$

Figure 3.4: Dimensionless temperature distribution (θ) of phase 1 and phase 2 (3).

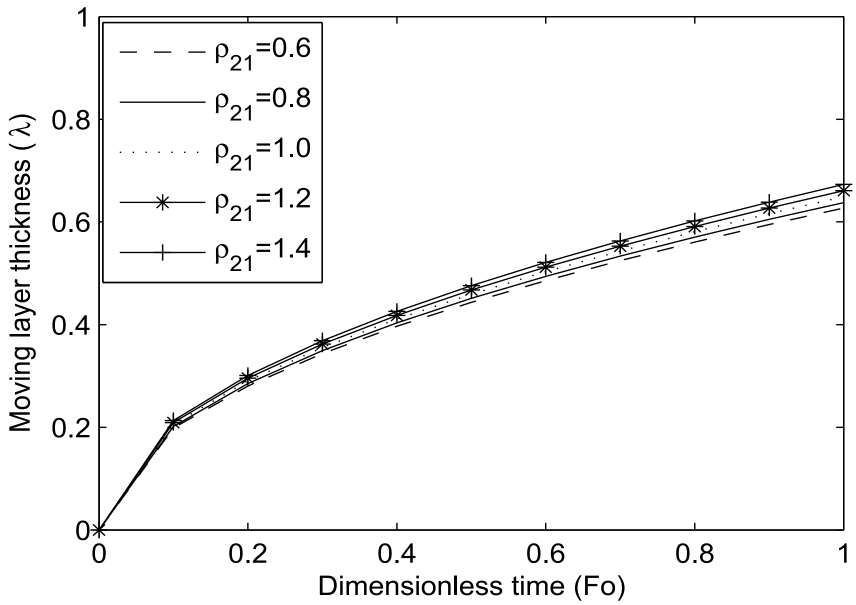

$a_{12} = 1$, $\theta_f = 0.5$, $\rho_{21} = 1$, $\alpha_1 = \alpha_2 = \beta_1 = \beta_2 = 0$

Figure 3.5: Effect of density (ρ_{21}) on moving layer thickness (λ).

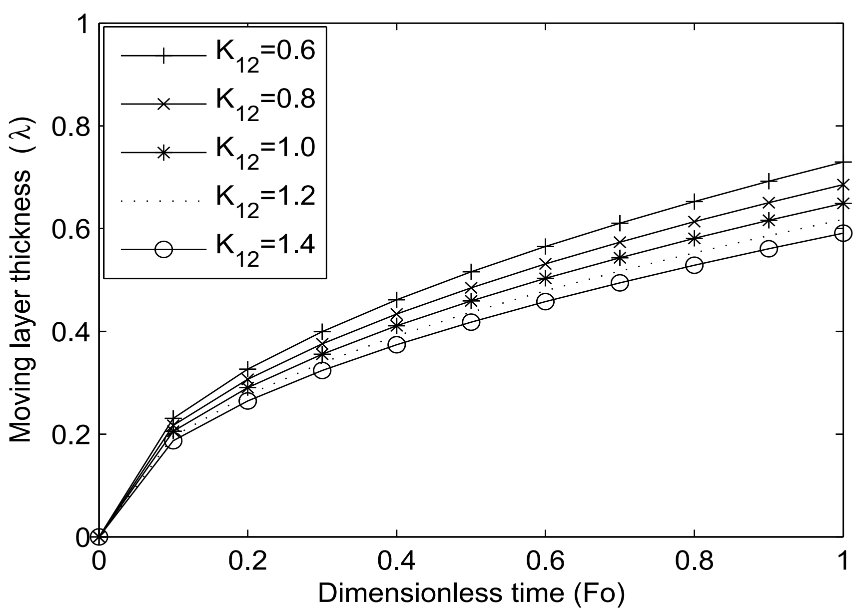

$a_{12} = 1$, $\theta_f = 0.5$, $\rho_{21} = 1$, $\alpha_1 = \alpha_2 = \beta_1 = \beta_2 = 0$

Figure 3.6: Effect of thermal conductivity (K_{12}) on moving layer thickness (λ).

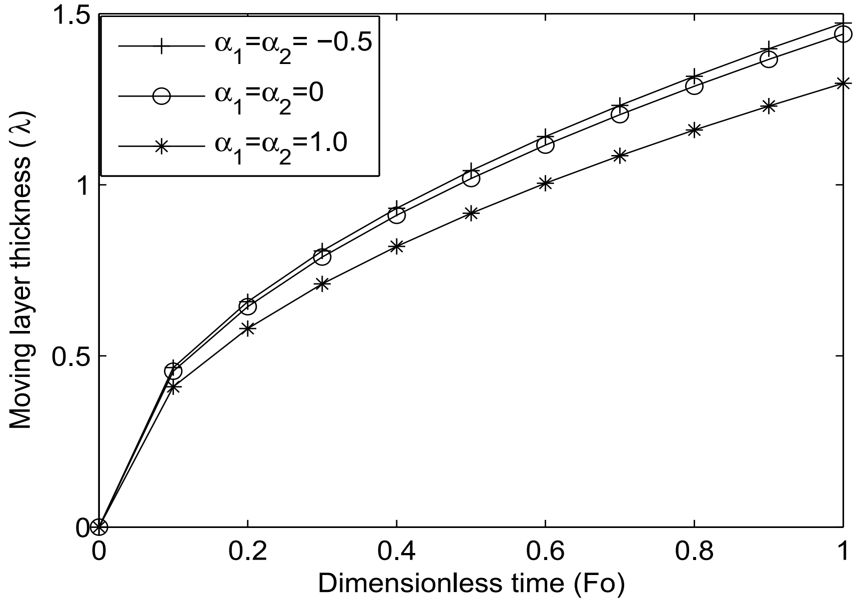

$a_{12} = 1,\ \theta_f = 0.5,\ \rho_{21} = 1,\ \beta_1 = \beta_2 = 1$

Figure 3.7: Effect of specific heat coefficients (α_1, α_2) on moving layer thickness (λ) in case (2).

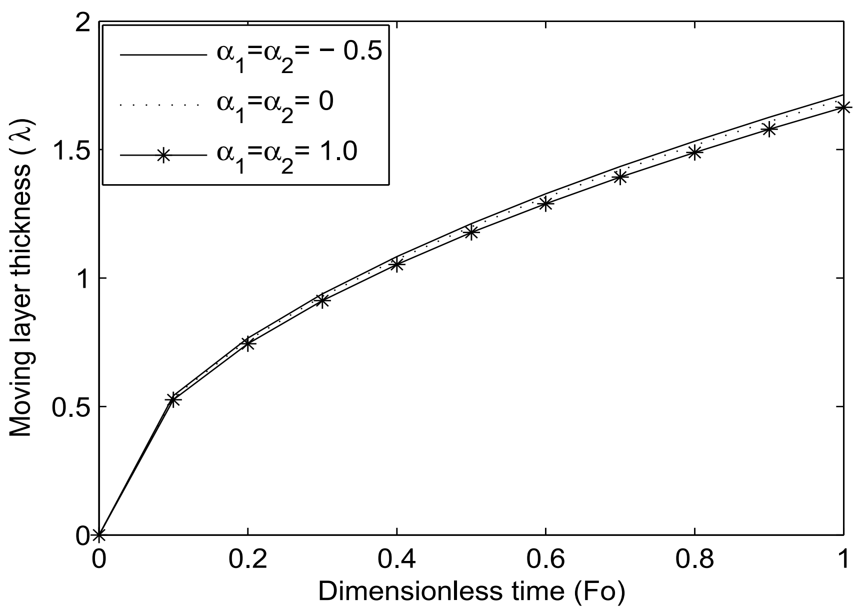

$a_{12} = 1,\ \theta_f = 0.5,\ \rho_{21} = 1,\ \beta_1 = \beta_2 = 1$

Figure 3.8: Effect of specific heat coefficients (α_1, α_2) on moving layer thickness (λ) in case (3).

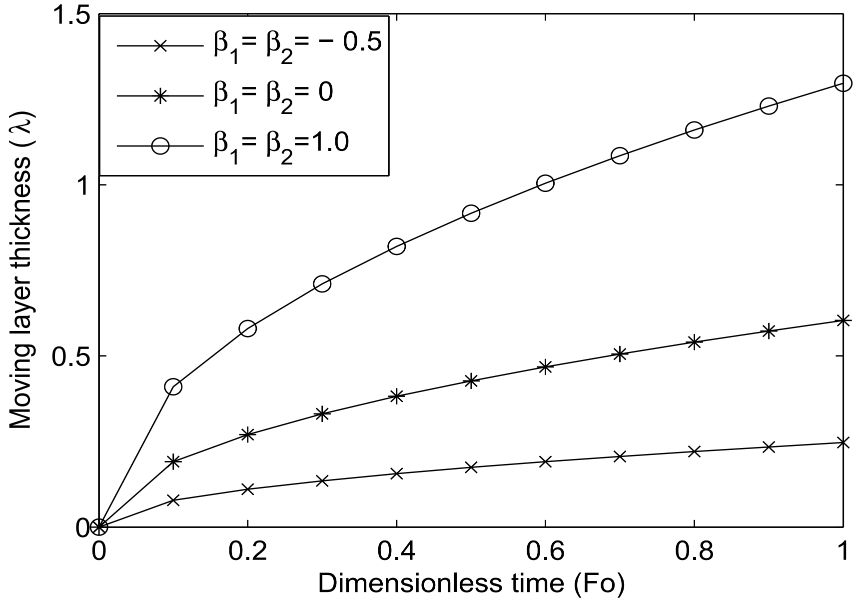

$a_{12} = 1$, $\theta_f = 0.5$, $\rho_{21} = 1$, $\alpha_1 = \alpha_2 = 1$

Figure 3.9: Effect of thermal conductivity coefficients (β_1, β_2) on moving layer thickness (λ) in case (2).

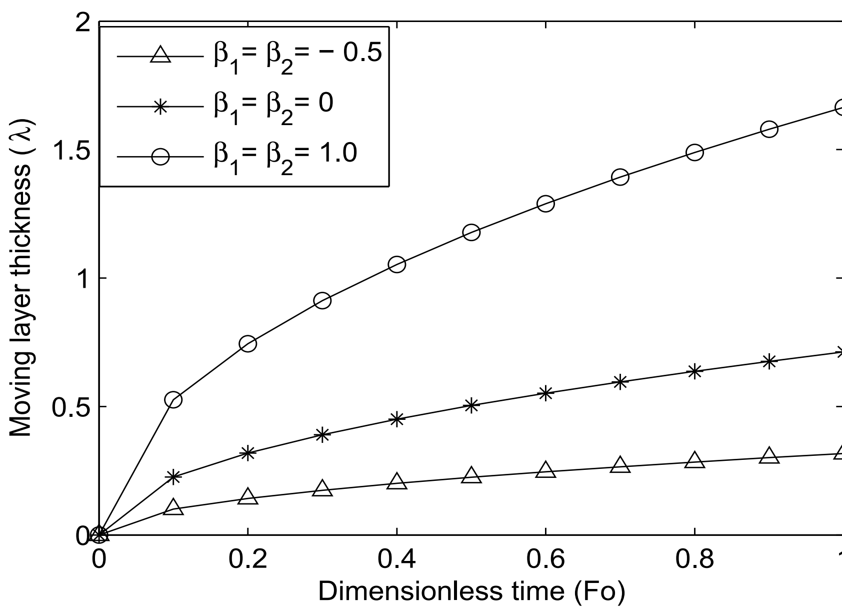

$a_{12} = 1$, $\theta_f = 0.5$, $\rho_{21} = 1$, $\alpha_1 = \alpha_2 = 1$

Figure 3.10: Effect of thermal conductivity coefficients (β_1, β_2) on moving layer thickness (λ) in case (3).

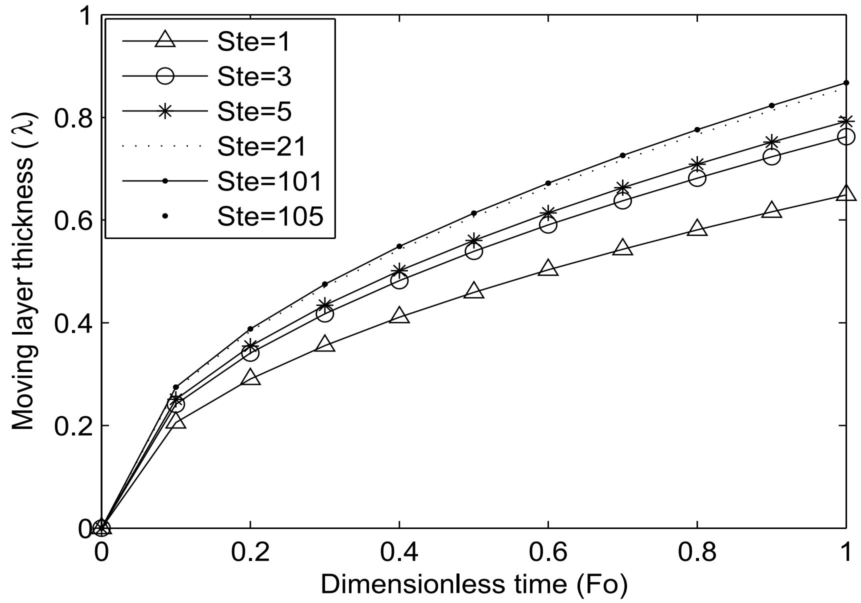

$a_{12} = 1$, $\theta_f = 0.5$, $\rho_{21} = 1$, $\alpha_1 = \alpha_2 = \beta_1 = \beta_2 = 0$

Figure 3.11: Effect of Stefan no. (Ste) on moving layer thickness (λ).

3.6 Conclusion

A mathematical model describing the process of freezing in a semi-infinite region has been analysed. The wavelet Galerkin and wavelet collocation methods are used to find the solution of moving boundary problem. The errors can be minimized and approaches to zero as the number of basis functions increase. This methodology is extremely efficient to provide the analytical solutions of moving boundary problems. The exceptional accuracy, prompts us to conclude that wavelet Collocation method may be excellent alternative to other methods for solving moving boundary problems. The temperature distribution in two regions and solid layer thickness can be accurately predicted with the wavelet Galerkin/wavelet Collocation solution. Our simulations show that

- as the ratio of thermal conductivity of liquid region to that of solid region increases, the moving layer thickness decreases while the ratio of density of liquid region to that of solid region increases, the moving layer thickness increases.

- the moving layer thickness increases as thermal conductivity increases with the temperature while decreases as heat capacity increases with temperature. The effect of thermal conductivity is more pronounced than heat capacity.

- as Stefan number increases, the thickness of solid layer increases and approaches to a constant value.